

**Stationary dynamics approach to analytical approximations for polymer coexistence curves**

S. M. Scheinhardt-Engels,\* F. A. M. Leermakers, and G. J. Fleer

*Laboratory of Physical Chemistry and Colloid Science, Wageningen University, Dreijenplein 6, 6703 HB Wageningen, The Netherlands*

(Received 15 August 2003; published 27 February 2004)

Phase separation in polymer blends is an important process. However, the compositions of the coexisting phases can only be predicted by numerical methods. We provide simple analytical expressions which serve as good approximations for the compositions after phase separation of binary homopolymer blends. These approximations are obtained by a stationary dynamics approach: we calculate the compositions of two polymer mixtures such that the stationary diffusion between these distinguishable mixtures vanishes. For the diffusion equations we employ composition-dependent diffusion coefficients, as derived according to the slow- and fast-mode theory from the Flory-Huggins free energy. The analytical results are in good agreement with exact (numerically calculated) binodal compositions. Our coexistence curves are more accurate than some conventional approximations. Another advantage of the stationary dynamics approach is that it is not only applicable to binary polymer blends or polymer solutions, but also to symmetrical multicomponent blends. The same diffusion coefficients may be used to obtain the exact spinodal compositions in multicomponent systems.

DOI: 10.1103/PhysRevE.69.021808

PACS number(s): 36.20.-r, 64.10.+h, 64.70.Ja

**I. INTRODUCTION**

Phase equilibria in polymer solutions and polymer blends are of great interest since in many instances different macromolecular species are combined to obtain materials with favorable properties. The implications of the phase behavior, such as the stability of polymer solutions and blends, is important not only in manufacturing and processing of materials, but also in their applications.

The great interest in the phase diagrams has led to a variety of simulation methods which were exclusively developed for the determination of coexistence curves. De Pablo *et al.* present a clear overview of the simulation methods [1]. One easy and robust way to obtain the compositions of coexisting phases is by Panagiotopoulos' Gibbs ensemble simulations [2,3]. This method needs  $n$  simulation boxes if  $n$  phases may coexist at the imposed temperature and overall composition. The Monte Carlo movements in the simulation allow subsequently the displacement of particles ( $NVT$  simulations), adjustment of the volumes ( $NPT$  simulations), and of the number of particles ( $\mu VT$  simulations) in each of these  $n$  boxes. The boxes are in contact due to the condition that particles and volume are exchanged, so that  $N$ ,  $V$ , and  $T$  are constant for the total of all boxes. Equilibrium is obtained when the pressure and chemical potentials are the same in all boxes. The computation time may be decreased by performing the simulation on a lattice, but then the volume exchanges need some extra attention [4,5]. The strength of the Gibbs ensemble method lies in the absence of interfaces: only bulk phases are simulated. One single simulation box containing two coexisting phases plus the interface in between would soon suffer from finite-size effects, especially near the critical point. However, problems arise in the Gibbs ensemble method when it is applied to macromolecules, since particle exchanges become extremely difficult. The acceptance probability of these exchanges may increase if

chains are inserted by a growth process, known as the configurational-bias method [6,7]. Other approaches to circumvent the insertion problem were proposed by Escobedo [8] and by Brennan and Madden [9]. The Gibbs ensemble simulation result is a good starting point for the Gibbs-Duhem integration scheme [10–12], which constitutes an efficient search for coexisting phases.

There are some attempts to find the coexistence curve by simulations in one cell only. The configurational-bias-vaporization method [13,14] and the adhesive-wall method [15] simulate the coexisting phases with their interface. The histogram reweighting method [16,17] is a powerful tool to find the coexistence curves by a limited number of simulations in which the interfaces need not be present.

This large number of attempts to find coexistence curves in polymer fluids indicates the importance of the issue. One general feature of such simulation methods is that one needs to start with a good estimate of the compositions of the coexisting phases. Such an initial guess might be obtained from a series of (time-consuming) trial simulations (e.g., by virtual Gibbs ensemble simulations [18]) or from simple analytical expressions. Some analytical expressions are available in the literature. We review them in the following section. In Sec. III we explain our “stationary dynamics approach” to obtain analytical approximations for coexistence curves. In this approach, we look for the compositions of two mixtures at which the stationary flux between these mixtures vanishes. We show that this approach in principle yields the exact binodal compositions when the equations are solved numerically. However, when the equations are solved analytically only an approximation is obtained due to the analytically inaccessible discontinuity in the diffusion profiles. We apply this approach to binary and symmetric multicomponent blends. Our analytical coexistence curves from the stationary dynamics approach are compared with other approximations and with exact results in Sec. IV. It is found that our approach, which is applicable for a wide range of polymer blends, yields better approximations than those available from literature. Spinodal curves are strongly related to the

\*Electronic address: Sonja.Engels@wur.nl

coexistence curves. Sec. V shows that the exact spinodals of binary and multicomponent polymer blends may be obtained from our flux expressions. Sec. VI summarizes our findings.

## II. ANALYTICAL BINODAL COMPOSITIONS

In this section, we focus on binary blends of homopolymers  $A$  and  $B$ . The approximations that are available from the literature apply the Flory-Huggins theory to find an expression for the chemical potential. This theory is simple and sometimes of limited use for experimental purposes, but it is still widely applied to understand phase behavior. It is used as a reference for newly developed models and it has served as the basis of new approaches [19–23]. Our stationary dynamics approach is not limited to the use of Flory-Huggins theory. We use this only to compare with the approximations available in the literature.

The free energy of mixing per lattice site for incompressible homopolymer mixtures in the Flory-Huggins model is

$$\frac{f}{k_B T} = \frac{g}{k_B T} + \text{const} = \sum_i \frac{\phi_i}{N_i} \ln \phi_i + \frac{1}{2} \sum_{i,j} \phi_i \chi_{ij} \phi_j. \quad (1)$$

Here,  $\phi_i$  and  $N_i$  denote the volume fraction and the chain length (that is, the number of constituent segments) of polymer  $i$ , respectively, and the parameters  $\chi_{ij}$  quantify the repulsive ( $\chi > 0$ ) or attractive ( $\chi < 0$ ) net interactions between segments  $i$  and  $j$ . Solvents are simply described as molecules with  $N=1$ . Due to the assumption of incompressibility, the Helmholtz ( $f$ ) and Gibbs ( $g$ ) free energies differ only by a constant.

We are looking for the binodal compositions, i.e., the volume fractions of both components in the two phases ( $\alpha$  and  $\beta$ ) that coexist at thermal equilibrium, for a given set of  $\chi$ 's. These compositions will be denoted, for polymer  $A$ , by  $\phi_A^\alpha$  and  $\phi_A^\beta$ . Thermal equilibrium implies equal chemical potentials in both phases:  $\mu_A^\alpha = \mu_A^\beta$  and  $\mu_B^\alpha = \mu_B^\beta$ . These chemical potentials follow from the standard procedure:  $\mu_A = \partial G / \partial n_A$ , where  $n_A$  is the number of  $A$  molecules. Using  $\phi_A = n_A N_A / (n_A N_A + n_B N_B)$  and  $G = (n_A N_A + n_B N_B) g$  it is then easy to obtain  $\mu_A / N_A = g + (1 - \phi_A)(\partial g / \partial \phi_A)$  so that

$$\frac{\mu_A}{k_B T} = \ln \phi_A + \left(1 - \frac{N_A}{N_B}\right) \phi_B + N_A \chi \phi_B^2, \quad (2)$$

where the pure phase  $A$  was taken as the reference point. The expression for  $\mu_B$  is obtained by interchanging the subscripts  $A$  and  $B$ . Obviously, in a binary mixture  $\phi_B = 1 - \phi_A$ . One relation between  $\phi_A^\alpha$  and  $\phi_A^\beta$  follows from  $\mu_A^\alpha = \mu_A^\beta$ :

$$\ln \frac{\phi_A^\alpha}{\phi_A^\beta} + \left(1 - \frac{N_A}{N_B}\right) (\phi_B^\beta - \phi_B^\alpha) + N_A \chi [\phi_A^\alpha (\phi_A^\alpha - 2) - \phi_A^\beta (\phi_A^\beta - 2)] = 0 \quad (3)$$

and a second relation, obtained from  $\mu_B^\alpha = \mu_B^\beta$ , is found by interchanging the subscripts  $A$  and  $B$  in Eq. (3) and substituting  $\phi_B = 1 - \phi_A$ . A numerical method is needed to find  $\phi_A^\alpha$  and  $\phi_A^\beta$  from these two relations. Even for the simplest

case of symmetrical polymer blends (i.e.,  $N_A = N_B = N$ ), which includes mixtures of monomers ( $N=1$ ), the binodal compositions are not analytically accessible. In this symmetrical case  $\phi_A^\beta = 1 - \phi_A^\alpha$  and Eq. (3) reduces to

$$\chi N = \frac{1}{2\phi_A^\alpha - 1} \ln \left( \frac{\phi_A^\alpha}{1 - \phi_A^\alpha} \right). \quad (4)$$

Numerical methods need good initial guesses to avoid divergence [24] for which analytical approximations are very helpful. We review three analytical approximations for the binodal compositions taken from the literature. Only one of these is generally applicable, the others are either for symmetrical blends ( $N_A = N_B = N$ ) or for polymer solutions ( $N_B = 1$ ) only. In the following discussion we need some extra quantities which may easily be derived from the Flory-Huggins free energy expression for a binary system. These are the spinodal compositions  $\phi_A^{\text{spin}} = 1 - \phi_B^{\text{spin}}$  that follow from the spinodal condition ( $\partial^2 G / \partial \phi^2 = 0$ ) and the critical composition and critical interaction parameter which are given by the critical condition ( $\partial^2 G / \partial \phi_A^2 = \partial^3 G / \partial \phi_A^3 = 0$ ):

$$\phi_A^{\text{spin}} = k \pm \frac{b}{\sqrt{2}}, \quad (5)$$

$$\phi_A^{\text{crit}} = k_{\text{crit}}, \quad (6)$$

$$\chi_{\text{crit}} = \frac{1}{2} \left( \frac{1}{\sqrt{N_A}} + \frac{1}{\sqrt{N_B}} \right)^2. \quad (7)$$

Here, we introduced parameters  $k$  and  $b$  defined by

$$k = \frac{1}{2} + \frac{1}{4\chi} \left( \frac{1}{N_A} - \frac{1}{N_B} \right) \quad (8)$$

$$b^2 = 2k^2 - \frac{1}{\chi N_A}. \quad (9)$$

The parameter  $k_{\text{crit}}$  is the value of parameter  $k$  after substitution of  $\chi = \chi_{\text{crit}}$  into Eq. (8):

$$k_{\text{crit}} = \frac{\sqrt{N_B}}{\sqrt{N_A} + \sqrt{N_B}}. \quad (10)$$

### A. Approximation for symmetrical blends

We first consider an analytical approximation for binodal compositions in blends that consist of two homopolymers with equal chain lengths ( $N_A = N_B = N$ ). The compositions are calculated by minimization of a Ginzburg-Landau expansion for the Flory-Huggins free energy [25]. The minimization is preceded by expanding the entropic contribution in terms of the order parameter  $\Psi = \phi - \phi^{\text{crit}}$ , which must be close to zero. This means that the system should be not far from its critical point. The minimization itself is carried out according to variational calculus. The result is therefore the coexistence curve according to a free energy functional that

merely serves as an upper bound for the real free energy. Here we are only interested in the approximation for the binodal compositions,

$$\phi^{vdw} = \frac{1}{2} \pm \sqrt{\frac{3}{8}(\chi N - 2)}, \quad (11)$$

but the procedure provides the complete composition profile between two liquid phases. It is known as the van der Waals theory of liquid/liquid interfaces.

### B. Approximation for polymer solutions

For a polymer  $A$  in a solvent  $B$  we have  $N_A = N$  and  $N_B = 1$ . The analytical approximation considered here provides only the binodal composition of the polymer-rich phase. The key element of this approximation is the assumption that the polymer-rich phase  $\beta$  coexists with a very dilute phase  $\alpha$  which is essentially pure solvent. In other words,  $\mu_B$  is assumed to be equal to zero in both phases so that the composition of the concentrated phase must obey

$$\frac{\mu_B^\beta}{k_B T} = \frac{\mu_B^\alpha}{k_B T} = \ln(1 - \phi_A^\beta) + \left(1 - \frac{1}{N}\right) \phi_A^\beta + \chi(\phi_A^\beta)^2 = 0. \quad (12)$$

This assumption results in an underestimation of the polymer content in the concentrated phase, in particular for small values of  $\chi$  and for chains that are relatively short. This can immediately be seen by inspection of  $\mu_B$  as a function of  $\phi_A$  [9]. An analytical approximation for Eq. (12) in the long-chain limit is obtained by neglecting the term  $1/N$  and expanding the logarithm, assuming small  $\phi_A$  even in the polymer-rich phase, which is valid for  $N \rightarrow \infty$  and small  $(\chi - \chi_{\text{crit}}) = (\chi - 1/2)$ . If the expansion is truncated after the term proportional to  $(\phi_A^\beta)^3$ , we obtain for the binodal composition of the polymer-rich phase:

$$\phi_A^{\text{sol}(i)} = 3\left(\chi - \frac{1}{2}\right). \quad (13)$$

Truncation after the next term still results in an analytical expression:

$$\phi_A^{\text{sol}(ii)} = \frac{2}{3} \left[ -1 + \sqrt{1 + 9\left(\chi - \frac{1}{2}\right)} \right]. \quad (14)$$

Due to the truncation, these approximations are overestimations of the underestimating Eq. (12). The result of this error compensation will be shown in Sec. IV. The assumption that a concentrated polymer solutions coexists with pure solvent forms the basis for an osmotic Gibbs ensemble simulation technique that circumvents the necessity for insertion and deletion of macromolecules [9].

### C. Approximation for all binary mixtures

Sanchez [26] has derived an approximation for Flory-Huggins coexistence curves that is valid both for symmetrical and asymmetrical binary blends as well as for polymer solutions. His derivation is based upon a Landau-type expan-

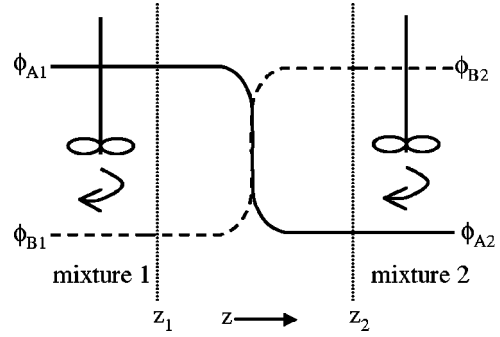


FIG. 1. Schematic picture of the system that is used to obtain approximations for binodal compositions: two ideally stirred mixtures in contact and a composition profile in between. There is no flux if the mixtures are coexistent at equilibrium.

sion of the free energy around the critical interaction parameter  $\chi^{\text{crit}}$  and the critical composition  $\phi_A^{\text{crit}}$ . He assumed that close to the critical point the binodal compositions are equidistant from the critical composition:  $\phi_A^\alpha - \phi_A^{\text{crit}} = \phi_A^\beta - \phi_A^{\text{crit}}$ . Combining the Landau expansion with this assumption, the equilibrium condition ( $\mu_A^\alpha = \mu_A^\beta$ ), and the spinodal condition ( $\partial^2 G / \partial \phi^2 = 0$ ) results in a simple relationship between the coexistence curve and the spinodal, which is known as the root-three rule:

$$\frac{\Delta \phi_A^{\text{bin}}}{\Delta \phi_A^{\text{spin}}} = \sqrt{3}, \quad (15)$$

where  $\Delta \phi_A^{\text{bin}} = \phi_A^{\alpha/\beta} - \phi_A^{\text{crit}}$  and  $\Delta \phi_A^{\text{spin}} = \phi_A^{\text{spin1/spin2}} - \phi_A^{\text{crit}}$ . Here,  $\phi_A^{\alpha/\beta}$  means either  $\phi_A^\alpha$  or  $\phi_A^\beta$ . Substituting Eqs. (5) and (6) into Eq. (15) yields for the root-three approximation for binodal compositions (denoted by  $\phi_A^{(\sqrt{3})}$ ):

$$\phi_A^{(\sqrt{3})} = k_{\text{crit}} + \sqrt{3}(k - k_{\text{crit}}) \pm \frac{1}{2} b \sqrt{6}. \quad (16)$$

### III. STATIONARY DYNAMICS APPROXIMATION

Our approach to find an approximation for the coexistence curve for given  $\chi$  is completely different from the approaches in Sec. II. We consider two polymer mixtures that differ in their compositions and that are brought into contact as shown in Fig. 1. It is assumed that these mixtures are infinitely large and ideally stirred, so that their compositions do not change in time. Generally, a diffusion flux will occur between these mixtures, driven by the concentration gradients, or, more precisely, by the chemical potential gradients. This is the key idea of our approach: *if the compositions of the mixtures are chosen such that the mixtures represent coexisting phases, there is no diffusion flux*. This statement cannot be inverted: the diffusion flux may also be absent for other compositions than that of coexisting phases, the trivial case being equal compositions for both mixtures. In the stationary situation, there is no accumulation of material within the contact zone between the two mixtures, and the fluxes are constant in time. Thus we can assign one value to the flux of each polymer in the stationary state. Our approach is to find those compositions that result in vanishing stationary fluxes

for all polymers. A similar idea forms the basis of a numerical algorithm to obtain phase diagrams [27]. The analytical approximations for binodal compositions that we find from this stationary dynamics approach (SDA) will be denoted by  $\phi_A^{\text{SDA}}$ .

We first need to derive expressions for the segment fluxes (Sec. III A), where we consider only one-dimensional diffusion perpendicular to the interface between the two mixtures. We will present the equations for stationary fluxes according to two different diffusion mechanisms. The assumptions about the diffusion mechanism are critical; they do not have an effect on the exact numerical results, but they determine whether it is possible to obtain an approximation for the coexistence curve.

The flux can be written in terms of Onsager coefficients and driving forces so that we generally have

$$J = -f(\phi)\nabla\mu \Leftrightarrow Jdz = -f(\phi)d\mu. \quad (17)$$

The function  $f(\phi)$  depends on the diffusion mechanism as will be seen in Sec. III B. In the stationary state, the flux is a constant so that integration of Eq. (17) from  $z=z_1$  to  $z=z_2$  yields for vanishing stationary fluxes

$$[z_2 - z_1]J^{\text{stat}} = - \int_{z_1}^{z_2} f(\phi)d\mu = 0. \quad (18)$$

At least one of the solutions of this equation yields the exact binodal compositions, independent of the function  $f(\phi)$ . This is because  $\int_{\mu=\alpha}^{\mu=\alpha} f(\phi)d\mu$  always equals zero; one of the solutions of Eq. (18) is found for  $\mu(z_1) = \mu(z_2)$ , which is the requirement for binodal compositions at  $z_1$  and  $z_2$ . However, an analytical approach requires the fluxes to be rewritten in terms of diffusion coefficients  $\tilde{D}$ :

$$[z_2 - z_1]J^{\text{stat}} = - \int_{z_1}^{z_2} \tilde{D}(\phi)d\phi = - \int_{z_1}^{z_2} f(\phi)\frac{\partial\mu}{\partial\phi}d\phi = 0. \quad (19)$$

Now the function  $f(\phi)$  determines (together with the chosen expression for the chemical potential) whether this equation can be solved analytically or not, and if it can be solved analytically, it determines the accuracy of the approximation. If the function  $f(\phi)$  is a constant, Eq. (19) requires a numerical calculation. If  $f(\phi)$  is not a constant, analytical solutions may be possible, but numerical calculations still yield the exact binodals, since Eq. (19) is equivalent to Eq. (18). The discrepancy between the numerical and analytical solutions of Eq. (19) originates from the shape of the volume fraction profiles between  $z_1$  and  $z_2$ ; numerical profiles show a discontinuity while the analytical profiles have a loop. This is shown in Fig. 2 for a binary system. The numerical profiles are calculated by the mean field stationary dynamics method [28] and the analytical profiles by solving Eq. (19) with the help of a simple form for the diffusion coefficient, presented later in Eq. (27). The analytical computation yields the inverse of the volume fraction profile  $z(\phi_A)$  instead of  $\phi_A(z)$ . Since analytical solutions will never yield the discontinuous jumps, we only obtain an approximation for the exact bin-

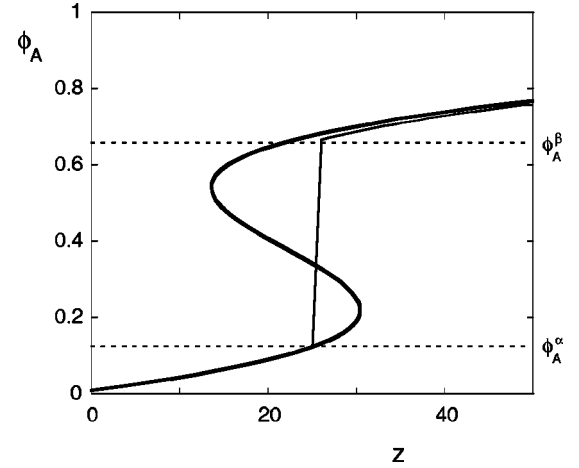


FIG. 2. Stationary volume fraction profiles between two stable mixtures calculated numerically (thin curve) and analytically (thick curve).  $N_A=30$ ,  $N_B=10$ ,  $\chi=0.14$ .

odals by analytically solving Eq. (19). The discontinuous jumps are a consequence of our simple definition for the segmental chemical potential, necessary for the analytical approach; this definition yields the correct value in the bulk phases but implies a simplification in the interfacial region. A more sophisticated expression of this potential, presented in Ref. [28], yields continuous profiles without any loop.

We will see in Sec. III B that Eqs. (18) or (19) is a sufficient condition for vanishing stationary fluxes between positions  $z_1$  and  $z_2$ , but only a necessary condition for coexisting phases at these positions. We will need an additional criterion for coexistence.

### A. Flux expressions

The expressions for the fluxes between polymer mixtures can be derived along the lines of the well-known fast-mode [29,30] and slow-mode [31] models. Experimentalists have tried to verify the predictions of each model, but there is no definite preference for any of them: some experiments are more consistent with the slow-mode model [32,33], others with the fast-mode model [34,35]. For a more detailed discussion, see Ref. [28].

The diffusion models were originally developed for binary blends, but may easily be generalized to multicomponent blends as shown in Ref. [28]. Here, we only present the results. In order to describe the diffusion on the scale of segments, the *segment* chemical potentials  $\mu^*$  are needed. They are simply calculated by dividing the chemical potential of a chain  $\mu$  by the number of chain segments  $N$ . This is an approximation since it is assumed that all segments of one chain have the same environment, although in the interfacial region the mixture is inhomogeneous on the length scale of the chain. In both diffusion models the segment fluxes satisfy the relation

$$\sum_i J_i = 0, \quad (20)$$

where the summation is taken over all segment types  $i$ . Ac-

cording to the slow-mode model, the system is incompressible and it is assumed that segments  $A$  diffuse by exchanging their positions with the positions of segments of type  $B, C, D, \dots$ . The fluxes are then given by

$$J_A^s = -\Lambda_A \nabla \mu_A^* + \frac{\Lambda_A}{\sum_i \Lambda_i} \sum_j \Lambda_j \nabla \mu_j^*. \quad (21)$$

The fast-mode model assumes that there is an additional flux of segments due to drift flow. This results in fluxes that are expressed by

$$J_A^f = -\Lambda_A \nabla \mu_A^* + \phi_A \sum_j \Lambda_j \nabla \mu_j^*. \quad (22)$$

The difference between these two equations is thus a different prefactor of  $\sum \Lambda \nabla \mu$ : the volume fraction in Eq. (22), and an ‘‘Onsager fraction’’ in Eq. (21). In the above equations  $\Lambda_A$  is an Onsager coefficient, which can be expressed in terms of the mobility coefficient  $\tilde{B}_A$  of segments  $A$ :

$$\Lambda_A(z) = \tilde{B}_A \phi_A(z). \quad (23)$$

The mobility coefficients may reflect the influence of entanglements on the dynamics of chains. This can be accounted for by considering the mobility coefficients to be a function of the monomer concentrations and chain lengths  $n$  [29,28]. However, in this study we consider the mobility coefficients  $\tilde{B}$  as being constant. Since we are interested in equilibrium properties of the blends, the choice of mobility coefficients should not be critical. In Sec. III C we explore the influence of segment mobilities on the approximations for binodal compositions. Note that the slow-mode and fast-mode expressions become identical if all segments have the same mobility  $\tilde{B}_A = \tilde{B}_B = \dots = \tilde{B}$ .

In the following we apply the stationary dynamics approach to binary and multicomponent blends. We simply use the Flory-Huggins expression for the segment chemical potential, since it allows direct comparison with the approximations discussed in Sec. II. In principle, any expression for the segment chemical potential could be chosen, as long as Eq. (19) can be solved analytically.

### B. Application to binary blends, $\tilde{B}_A = \tilde{B}_B$

We first apply the stationary dynamics approach to binary blends. For binary blends with  $\tilde{B}_A = \tilde{B}_B = \tilde{B}$  we have according to Eqs. (21) and (22)

$$J_A^s = J_A^f = -\tilde{B} \phi_A \phi_B \nabla (\mu_A^* - \mu_B^*). \quad (24)$$

Thus a vanishing stationary flux corresponds to

$$\begin{aligned} J_A^{\text{stat},s} = J_A^{\text{stat},f} &= -\frac{\tilde{B}}{[z_2 - z_1]} \int_{z_1}^{z_2} \phi_A \phi_B d(\mu_A^* - \mu_B^*) \\ &= -\frac{\tilde{B}}{[z_2 - z_1]} \int_{z_1}^{z_2} \phi_A d\mu_A^* = 0. \end{aligned} \quad (25)$$

For the third equality we used the Gibbs-Duhem equation ( $\sum_i \phi_i d\mu_i = 0$ ) and  $\phi_A + \phi_B = 1$ . We see that the flux vanishes if  $\mu_A^*(z_1) - \mu_B^*(z_1) = \mu_A^*(z_2) - \mu_B^*(z_2)$ , or in other words if  $\Delta \mu_A^* = \Delta \mu_B^*$ , where  $\Delta \mu^* = \mu^*(z_2) - \mu^*(z_1)$ . This occurs (i) if mixtures 1 and 2 are identical, (ii) if they are coexistent or, (iii) if the driving force for diffusion of segments  $A$  is nonzero and the same (equal and in the same direction) as for segments  $B$ . In the third scenario none of the segments will be able to diffuse due to the incompressibility constraint [Eq. (20)]. This scenario can only occur if at least one of the two mixtures is not stable (i.e., inside the binodal), since different stable mixtures always have different chemical potentials if the mixtures are noncoexistent.

Comparing Eq. (25) with Eq. (18) we find that in this case the function  $f(\phi)$  in Eq. (18) is given by

$$f(\phi_A) = \tilde{B} \phi_A, \quad (26)$$

and by using Eq. (19) and the Flory-Huggins chemical potential we find for  $\tilde{D}(\phi)$ :

$$\frac{\tilde{D}(\phi_A)}{k_B T} = f(\phi_A) \frac{\partial \mu_A^*}{\partial \phi_A} \frac{1}{k_B T} = \tilde{B} \phi_A \phi_B \left( \frac{1}{\phi_A N_A} + \frac{1}{\phi_B N_B} - 2\chi \right). \quad (27)$$

The function  $f(\phi_A)$  is linear in  $\phi_A$ , which allows an analytical expression for the stationary flux according to  $J = -\int \tilde{D} d\phi_A$ :

$$\begin{aligned} J_A^{\text{stat}} = \tilde{C}(\phi_{A1} - \phi_{A2}) [ &\phi_{A1}^2 + \phi_{A1} \phi_{A2} + \phi_{A2}^2 - 3k(\phi_{A1} + \phi_{A2}) \\ &+ 3k^2 - \frac{3}{2}b^2], \end{aligned} \quad (28)$$

where  $\tilde{C} = \frac{2}{3} \tilde{B} \chi k_B T / [z_2 - z_1]$ . There may exist many combinations of  $\phi_{A1}$  and  $\phi_{A2}$  for which the stationary flux vanishes. One of these combinations is the trivial case of identical blends ( $\phi_{A1} = \phi_{A2}$ ), another combination must be the coexisting blends ( $\phi_{A1} = \phi_A^\alpha$  and  $\phi_{A2} = \phi_A^\beta$  or vice versa), the remaining combinations must have either  $\phi_A^\alpha < \phi_{A1} < \phi_A^\beta$  or  $\phi_A^\alpha < \phi_{A1} < \phi_A^\beta$  or both.

To find the best approximation for coexisting phases at  $z_1$  and  $z_2$ , we need an extra criterion in addition to the requirement

$$\phi_{A1}^2 + \phi_{A1} \phi_{A2} + \phi_{A2}^2 - 3k(\phi_{A1} + \phi_{A2}) + 3k^2 - \frac{3}{2}b^2 = 0, \quad (29)$$

in particular for  $N_A \neq N_B$ . Therefore it is convenient to inspect the general plot of the stationary flux vs the composition of mixture 2 for given  $\phi_{A1}$  (see Fig. 3). If both mixtures are stable, we have  $J_A^{\text{stat}} > 0$  (diffusion to the right) for  $\phi_{A2} < \phi_{A1}$  and  $J_A^{\text{stat}} < 0$  (diffusion to the left) for  $\phi_{A2} > \phi_{A1}$ . If

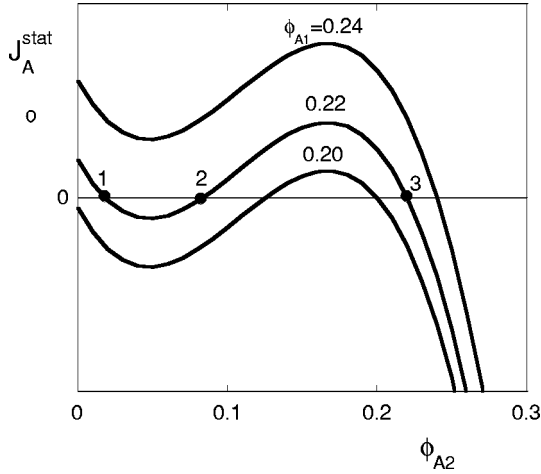


FIG. 3. Analytically calculated stationary flux as function of the composition of mixture 2 for different compositions of mixture 1, as indicated by the value of  $\phi_{A1}$ .  $N_A=100$ ,  $N_B=1$ ,  $\chi=0.63$ .

one of the mixtures is unstable (inside the binodal curve) the stationary flux may be negative for  $\phi_{A2} < \phi_{A1}$  and positive for  $\phi_{A2} > \phi_{A1}$  depending on the chemical potentials of all components. Differentiating Eq. (28) with respect to  $\phi_{A2}$  at constant  $\phi_{A1}$  gives  $\partial J_A^{\text{stat}} / \partial \phi_{A2} = 0$  when  $\phi_{A2} = k \pm b / \sqrt{2}$ . Comparing this with Eq. (5), we see that the minimum and maximum in Fig. 3 correspond to the spinodal composition of mixture 2. Also,  $\partial^2 J_A^{\text{stat}} / \partial \phi_{A2}^2 = 0$  for  $\phi_{A2} = k$ ; the inflection point lies halfway the two local extrema. Hence, the position of the two extrema and the inflection point in between do not depend on  $\phi_{A1}$ . In fact, upon changing  $\phi_{A1}$  the curves translate vertically, as follows from Eq. (28).

Depending on the choice for  $\phi_{A1}$  the curve has either one, two, or three zero points. These points are indicated by the numbers 1, 2, and 3 for  $\phi_{A1} = 0.22$ . Point 3 corresponds to  $\phi_{A2} = \phi_{A1}$ , points 1 and 2 can be found by solving the quadratic equation (29). If mixture 1 has a binodal composition ( $\phi_{A1} = \phi_A^\alpha$ ) the three zero points are  $\phi_{A2} = \phi_A^\alpha$  (point 3),  $\phi_{A2} = \phi_A^\beta$  (point 1), and  $\phi_A^\beta < \phi_{A2} < \phi_A^\alpha$  (point 2). This zero point 2 gives the necessary condition for coexisting phases in addition to Eq. (29). It must represent the situation that  $\Delta \mu_A^* = \Delta \mu_B^* \neq 0$ . The additional condition is that  $\phi_{A2}$  must have a certain given value (that of zero point 2), so that Eq. (29) is obeyed only if mixture 1 has a binodal composition. We look for the appropriate value of zero point 2 in Sec. III B 2 after exploring the approximation for symmetrical systems in the following section.

### 1. $\bar{B}_A = \bar{B}_B$ and $N_A = N_B$

In a symmetrical binary blend, both components have the same chain length. For such systems, we do not explicitly need the plot of  $J_A^{\text{stat}}$  vs  $\phi_{A2}$ : the extra criterion for coexistence is simply  $\phi_A^\beta = \phi_B^\alpha = 1 - \phi_A^\alpha$ . Substitution of  $\phi_{A2} = 1 - \phi_{A1}$  and  $N_A = N_B = N$  into Eq. (29) yields the analytical approximation for binodal compositions in symmetrical binary blends in which  $\bar{B}_A = \bar{B}_B$ :

$$\phi_A^{\text{SDA}} = k \pm \frac{1}{2} b \sqrt{6} = \frac{1}{2} \pm \sqrt{\frac{3\chi N - 6}{4\chi N}}. \quad (30)$$

For symmetrical blends  $k = k_{\text{crit}} = \frac{1}{2}$ , so that for these blends our approximation is identical to the root-three rule approximation [Eq. (16)].

Although we did not need the plot of  $J_A^{\text{stat}}$  vs  $\phi_{A2}$  for the additional criterion, we can of course still relate this plot to  $\phi_A^{\text{SDA}}$ . The inflection point of  $J_A^{\text{stat}}(\phi_{A2})$  for symmetrical blends does not only lie exactly halfway the spinodal compositions, but also halfway the binodal compositions, since  $|\phi_A^\alpha - \phi_A^{\text{spin}1}| = |\phi_A^\beta - \phi_A^{\text{spin}2}|$ . In other words for symmetrical systems the zero point 2 in Fig. 3 is also the inflection point. Thus for symmetrical blends the stationary flux vanishes if mixture 1 has a binodal composition, and mixture 2 has either the same composition (point 3), or the coexisting composition (point 1), or the composition of the inflection point ( $\phi_{A2} = k$ , point 2). Hence, instead of selecting  $\phi_{A2} = 1 - \phi_{A1}$  as the additional criterion, we could have selected  $\phi_{A2} = k$ . Indeed, substitution of  $\phi_{A2} = k = k_{\text{crit}} = \frac{1}{2}$  into Eq. (29) yields the same approximation for the binodal compositions as presented by Eq. (30).

### 2. $\bar{B}_A = \bar{B}_B$ and $N_A \neq N_B$

We do not have a simple relation between  $\phi_A^\alpha$  and  $\phi_A^\beta$  for  $N_A \neq N_B$  which could be used as the necessary criterion in addition to Eq. (29). We propose two alternative additional criteria for vanishing fluxes if mixture 1 has a binodal composition:  $\phi_{A2} = k$  or  $\phi_{A2} = k_{\text{crit}}$ . For  $N_A = N_B$  these criteria are identical and they yield the approximation as presented in Eq. (30). Both criteria obey the requirement that  $J_A^{\text{stat}}(\phi_{A2})$  has three intersections with the line  $J_A^{\text{stat}} = 0$  if mixture 1 has a binodal composition, since both  $k$  and  $k_{\text{crit}}$  are somewhere between the two spinodal compositions which correspond to the local extrema of the curve.

The first choice for the additional criterion ( $\phi_{A2} = k$ ) is related to the inflection point of  $J_A^{\text{stat}}(\phi_{A2})$ . By taking this criterion, we assume that we must vertically translate the curve  $J_A^{\text{stat}}(\phi_{A2})$  until the inflection point is also a zero point of  $J_A^{\text{stat}}$ . The other zero points are then supposed to be the binodal compositions.

The alternative choice for the additional criterion ( $\phi_{A2} = k_{\text{crit}} = \phi_A^{\text{crit}}$ ) is related to the observation in Eq. (25) that the stationary flux vanishes if  $\Delta \mu_A^* = \Delta \mu_B^*$ . By taking this criterion we assume that both components in a mixture with a binodal composition feel the same driving force for diffusion when the other mixture has a critical composition. This is equivalent to the assumption that the chemical potential difference between the two components  $\mu_A^* - \mu_B^*$  is equal in the binodal and the critical compositions.

We also based the selection of these two criteria on numerical calculations of the stationary flux. By use of the mean field stationary dynamics method [28] the flux can be calculated exactly according to Eq. (18). In these numerical calculations (also based upon the Flory-Huggins free energy functional), mixture 1 was kept at the binodal composition  $\phi_A^\alpha$ . We varied the composition of mixture 2 between  $\phi_{A2}$

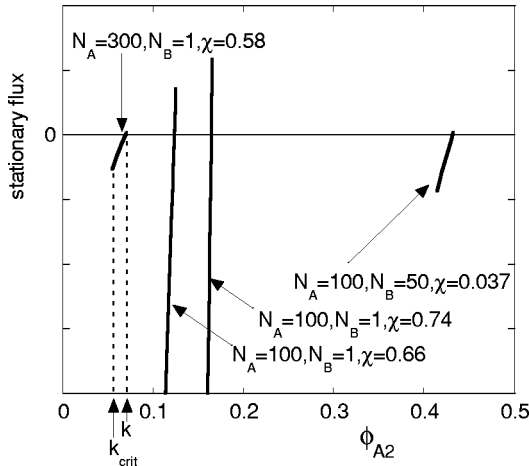


FIG. 4. The exact stationary flux between two mixtures for four different systems. In all systems, one mixture ( $\phi_{A1}$ ) has a binodal composition. The composition  $\phi_{A2}$  of the other mixture increases from  $k_{\text{crit}}$  to  $k$ . For the four combinations of  $N_A$ ,  $N_B$ , and  $\chi$  given in the figure (from left to right)  $k_{\text{crit}} = 5.46 \times 10^{-2}$ ,  $9.09 \times 10^{-2}$ ,  $9.09 \times 10^{-2}$ ,  $0.414$  and  $k = 7.04 \times 10^{-2}$ ,  $0.125$ ,  $0.166$ ,  $0.432$ . The exact stationary flux always vanishes for some value of  $\phi_{A2}$  in between these limits.

$=k_{\text{crit}}$  and  $\phi_{A2}=k$ . Figure 4 presents the results for various systems with  $N_A > N_B$  and  $\tilde{B}_A = \tilde{B}_B$ . Each curve is in fact part of a curve as presented in Fig. 3, viz. the part close to point 2. The two main intersections with the horizontal axis would occur for  $\phi_{A2} = \phi_A^\alpha$  and  $\phi_{A2} = \phi_A^\beta$ . Indeed, the third intersection of the stationary flux with the horizontal axis occurs for  $k_{\text{crit}} < \phi_{A2} < k$ .

To select the best of our two additional criteria, we observe that the first ( $\phi_{A2}=k$ ) yields the same result as obtained in Eq. (30):  $\phi_A^{\text{SDA}} = k \pm \frac{1}{2}b\sqrt{6}$ . A weak aspect of this criterion is that the resulting binodal compositions are both equally far from the spinodal compositions, which is not true for real binodal compositions. We therefore select the alternative ( $\phi_{A2}=k_{\text{crit}}$ ) as the necessary condition for a binodal composition of the mixture at the right hand side. Substitution of  $\phi_{A2}=k_{\text{crit}}$  into Eq. (29) yields the stationary dynamics approximation for binodal compositions in binary blends with  $N_A \neq N_B$  and  $\tilde{B}_A = \tilde{B}_B$ :

$$\phi_A^{\text{SDA}} = \frac{1}{2} [3k - k_{\text{crit}} \pm \sqrt{6b^2 - 3(k - k_{\text{crit}})^2}]. \quad (31)$$

We have compared this approximation with the approximation obtained from  $\phi_{A2}=k$  in plots similar to those to follow in Sec. IV. Indeed,  $\phi_{A2}=k_{\text{crit}}$  yields a better approximation than  $\phi_{A2}=k$  although the numerically calculated flux has zero point 2 closer to  $k$  than to  $k_{\text{crit}}$ .

### C. Application to binary blends, $\tilde{B}_A \neq \tilde{B}_B$

The segment mobilities enter the expressions for the stationary flux via the function  $f(\phi)$ , and may thereby determine whether an analytical prediction of the binodal compositions is possible or not.

### 1. Slow-mode diffusion mechanism

From Eq. (21) we find for the slow-mode flux

$$[z_2 - z_1] J_A^{\text{stat},s} = -\tilde{B}_A \tilde{B}_B \int_{z_1}^{z_2} \frac{\phi_A \phi_B}{\tilde{B}_A \phi_A + \tilde{B}_B \phi_B} d(\mu_A^* - \mu_B^*). \quad (32)$$

The function  $f(\phi_A)$  is found by applying the Gibbs-Duhem equation to Eq. (32):

$$f(\phi_A) = \tilde{B}_A \tilde{B}_B \frac{\phi_A}{\phi_A(\tilde{B}_A - \tilde{B}_B) + \tilde{B}_B}. \quad (33)$$

This function does not allow the analytical solution of  $J^{\text{stat}} = -\int \tilde{D} d\phi = 0$ , in contrast to the function  $f(\phi)$  in Eq. (26), which is linear in  $\phi_A$  and follows from Eq. (33) by substituting  $\tilde{B}_A = \tilde{B}_B$ .

If segments  $B$  are almost immobile compared to segments  $A$ , i.e., in the limit of  $\tilde{B}_A/\tilde{B}_B \rightarrow \infty$ , we obtain  $f(\phi_A) \rightarrow \tilde{B}_B$ . The diffusion may thus be described by the diffusion of only one (the slowest) component. Density gradients are immediately relaxed by the other component. Since  $f(\phi_A)$  is a constant,  $J^{\text{stat}} = -\int \tilde{D} d\phi$  would again require a numerical calculation. In the limit of  $\tilde{B}_B/\tilde{B}_A \rightarrow \infty$  it is found that  $f(\phi_B) \rightarrow \tilde{B}_A$ .

### 2. Fast-mode diffusion mechanism

The fast-mode stationary flux for binary systems is given by

$$[z_2 - z_1] J_A^{\text{stat},f} = -\tilde{B}_A \int_{z_1}^{z_2} \phi_A \phi_B d\mu_A^* + \tilde{B}_B \int_{z_1}^{z_2} \phi_A \phi_B d\mu_B^*, \quad (34)$$

so that we find for  $f(\phi_A)$

$$f(\phi_A) = \tilde{B}_A \phi_A + (\tilde{B}_B - \tilde{B}_A) \phi_A^2. \quad (35)$$

In combination with the Flory-Huggins potentials, this function only provides an analytical solution for  $J^{\text{stat}} = -\int \tilde{D} d\phi = 0$  if  $N_A = N_B$ .

### D. Application to symmetrical multicomponent blends

We now consider symmetrical systems containing  $K$  components. The symmetry in these systems arises from requirements on chain lengths and interaction parameters:  $N_i = N \forall i$  and  $\chi_{ij} = \chi \forall i, j \neq i$ . Moreover, we assume  $\tilde{B}_i = \tilde{B} \forall i$ . At the corners of the  $K$ -phase region the volume fractions of  $(K-1)$  components are equal to  $\phi^{\text{co}}$ , and one component has volume fraction  $1 - (K-1)\phi^{\text{co}}$ . It is our aim to find  $\phi^{\text{co}}$  as function of  $\chi N$ . The exact solution is numerically available from [36]:

$$\frac{1}{1 - K\phi^{\text{co}}} \ln \left[ \frac{1}{\phi^{\text{co}}} - (K-1) \right] = \chi N. \quad (36)$$

For our approach we write the flux by use of either Eq. (21) or (22) and the Gibbs-Duhem equation as

$$J_A = -\tilde{B}\phi_A\nabla\mu_A^* = -\sum_i f(\phi_A)\left(\frac{\partial\mu_A^*}{\partial\phi_i}\right)_{\phi_{j\neq i,n}}\nabla\phi_i. \quad (37)$$

In analogy to the approach for binary blends, we find for the mutual diffusion coefficients  $\tilde{D}_{Ai}^{(K)}$ , defined by  $J_A = -\sum_i\tilde{D}_{Ai}^{(K)}\nabla\phi_i$ :

$$\frac{\tilde{D}_{Ai}^{(K)}}{\tilde{B}k_B T} = \phi_A\phi_i\chi - \phi_A\phi_K\chi + (\delta_{AK} - \delta_{Ai})\left(\phi_A\chi - \frac{1}{N}\right). \quad (38)$$

The Kronecker delta  $\delta_{AB}$  equals unity for  $A=B$  and is zero otherwise. The superscript  $(K)$  indicates that  $\phi_K$  is written as  $1 - \sum_{i\neq K}\phi_i$ , which is necessary in the calculation of the total differential in Eq. (37).

We assume that we should always find the same compositions for the coexisting phases independent on the profiles of components  $B, C, \dots, K-1$  at the interface between these phases. In other words, we substitute  $\nabla\phi_i=0$  for all  $i\neq A, K$  into Eq. (37) so that  $J_A = -\tilde{D}_{AA}^{(K)}\nabla\phi_A$ . We need to calculate  $\phi^{\text{co}}$  for which  $\int_{z_1}^{z_2}\tilde{D}_{AA}^{(K)}d\phi_A=0$ . After the integration we substitute  $\phi_{A1}=\phi_{K2}=\phi^{\text{co}}$ ,  $\phi_{A2}=\phi_{K1}=1-(K-1)\phi^{\text{co}}$  and  $\phi_{i1}=\phi_{i2}=\phi^{\text{co}}\forall i\neq A, K$ . Again [as for the binary systems, Eq. (28)] the result is a cubic equation in  $\phi^{\text{co}}$ . One root of this polynomial is known: the flux should at least vanish if all components have the same volume fractions, thus  $\phi^{\text{co}}=1/K$ . The two remaining roots are then found to be

$$\phi^{\text{co}} = \frac{1}{2K^2}\left\{6-K \pm \sqrt{3K^2\left(3-\frac{8}{\chi N}\right) + 12(3-K)}\right\}. \quad (39)$$

Only one of these two roots is a valid approximation [unless  $K=2$  for which  $\phi^{\text{co}}$  reduces to Eq. (30)]. Since the  $K$ -phase region increases with  $\chi N$ ,  $\phi^{\text{co}}$  must decrease with  $\chi N$ . We must therefore use the minus sign in Eq. (39).

We can also find approximations for the compositions at the corners of  $(K-1)$ -phase regions (for  $K>2$ ). At these corners, one minority component has volume fraction  $\phi^{\text{m}}$ ,  $(K-2)$  components have volume fractions  $\phi^{\text{co}}$ , and the volume fraction of the last component is  $1-\phi^{\text{m}}-(K-2)\phi^{\text{co}}$ . We want to obtain  $\phi^{\text{co}}$  as a function of  $\phi^{\text{m}}$  and  $\chi N$ . The exact solution can be calculated numerically from [36]

$$\frac{1}{1-\phi^{\text{m}}-(K-1)\phi^{\text{co}}}\ln\left[\frac{1-\phi^{\text{m}}}{\phi^{\text{co}}}-K+2\right]=\chi N. \quad (40)$$

Taking the integral of the mutual diffusion coefficient and substituting two corner compositions into the result yields a cubic equation in  $\phi^{\text{co}}$ . One root is given by  $\phi^{\text{co}}=(1-\phi^{\text{m}})/(K-1)$ . The others are

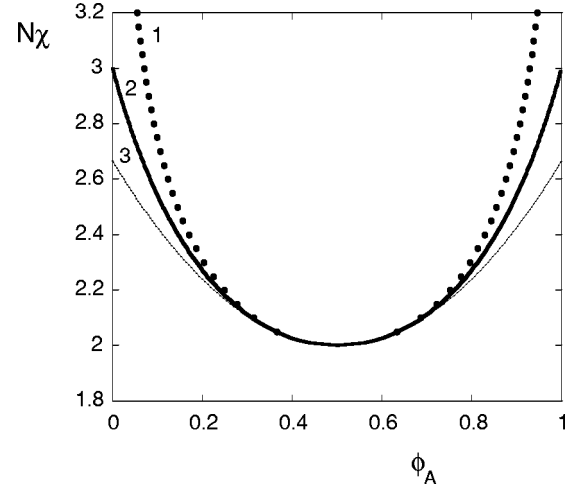


FIG. 5. Comparison of exact and approximated coexistence curves for binary homopolymer systems with  $N_A=N_B=N$ . Curve 1 is the exact binodal [Eq. (4)], curve 2 is our analytical approximation [Eq. (30)], which in this case equals the root-three rule approximation [Eq. (16)], curve 3 is the analytical van der Waals approximation [Eq. (11)].

$$\phi^{\text{co}} = \frac{\phi^{\text{m}}}{1-K} + \frac{1}{2(K-1)^2}\left\{7-K \pm \sqrt{24(1-K)\phi^{\text{m}} + (7-K)^2 + 8(K-1)^2\left(1-\frac{3}{\chi N}\right)}\right\}. \quad (41)$$

This reduces to Eq. (39) for  $\phi^{\text{m}}=\phi^{\text{co}}$ .

## IV. RESULTS

The performance of our approximations for the binodal compositions can easily be evaluated by comparing them with the numerically calculated binodal and with other approximations. In this section, we only consider our approximations for systems with equal segment mobilities for all components, so that the fast- and slow-mode models are identical.

### A. Symmetric binary blends

In Fig. 5 we have plotted three binodals (coexistence curves). The use of the variable  $\chi N$  allows to cover all possible symmetrical binary systems at once. Curve 1 is the exact binodal, curve 2 is our approximation [Eq. (30)], which in this case equals the root-three rule approximation, and curve 3 is the approximation obtained by the van der Waals theory of fluid interfaces [Eq. (11)]. It is seen that all approximations perform well for systems not too far from their critical point ( $\chi N=2$ ) and that our approximation (or the root-three rule) is significantly more accurate than van der Waals' approximation for larger  $\chi N$ .

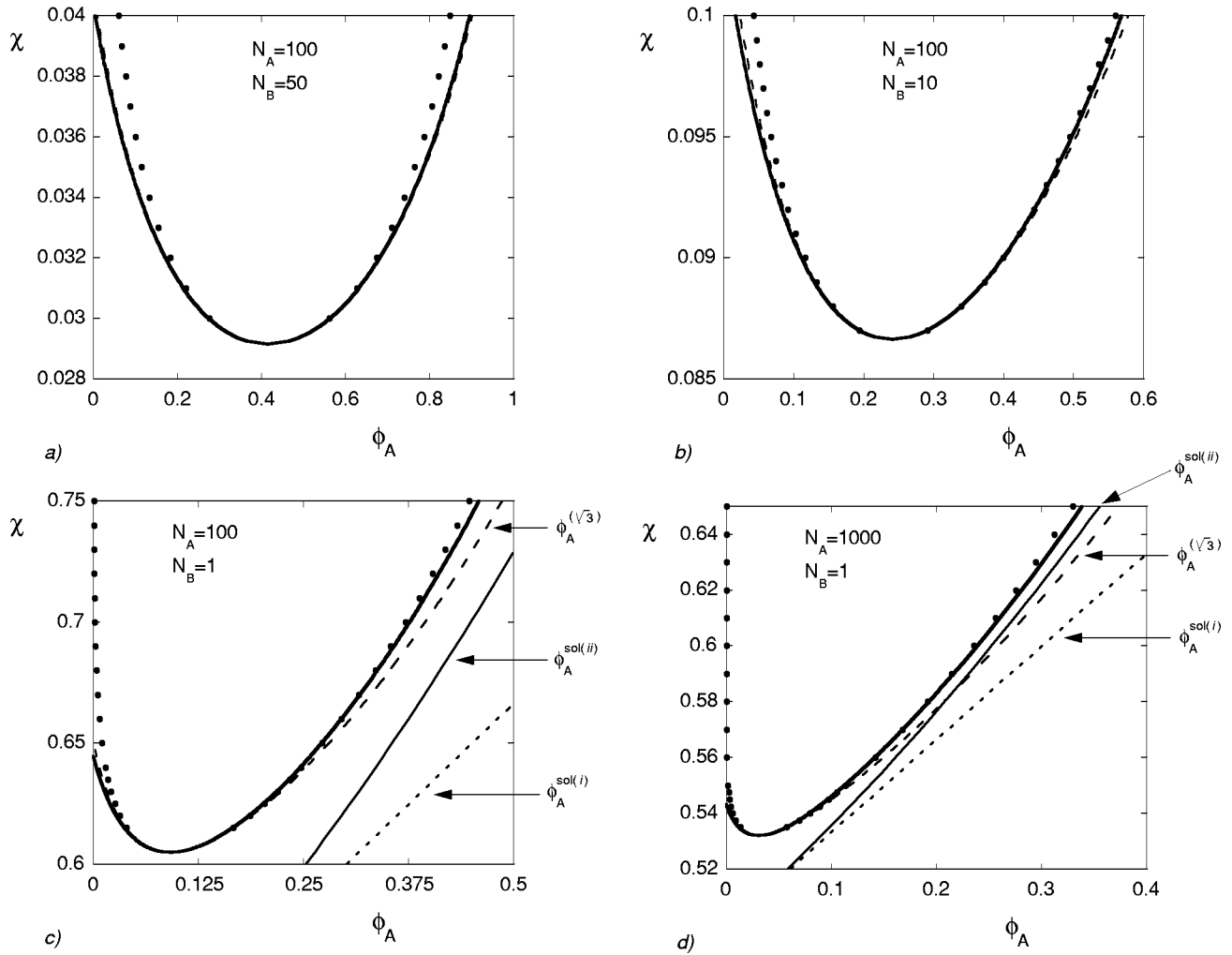


FIG. 6. Comparison of our approximation, Eq. (31), (thick solid curves) with the exact binodal (dots), the root-three rule of Eq. (16) (dashed curves), and the solution approximations of Eqs. (13) and (14) (dotted and thin solid curves, respectively).

### B. Asymmetrical binary blends

Figures 6(a)–6(d) illustrate the performance of our approximation for some typical examples of asymmetrical binary blends. The dots in these figures always represent the exact binodals, the solid curves correspond to our approximation given by Eq. (31), and the dashed curves to the root-three rule. In Fig. 6(a) the chain lengths do not differ too much, and our approximation almost coincides with the root-three result. Moreover, the accuracy of our approximation is comparable to that for symmetrical systems. With increasing  $N_A/N_B$  the discrepancy between our approximation and the root-three result increases, in particular for the branch of the coexistence curve that corresponds to the phase that is relatively rich in the longer chains. Our approximation is more accurate for this branch. For the other branch (dilute in the longer chains), the root-three rule is slightly more accurate than our approximation, but the difference is very small. Both approximations for the diluted branch fail for high  $\chi$ , since they predict negative volume fractions.

We can also compare our approximation with the approximations for polymer solutions [Eqs. (13) and (14)]. In Figs. 6(c) and 6(d) ( $N_B=1$ ), where the polymer in solution has

chain lengths 100 and 1000, respectively, we see that our approximation is much more accurate than  $\phi_A^{\text{sol}(i)}$  and  $\phi_A^{\text{sol}(ii)}$  (dotted lines). The accuracies of  $\phi_A^{\text{sol}(i)}$  and  $\phi_A^{\text{sol}(ii)}$  increase with  $N_A$ . We may substitute  $N_A \rightarrow \infty$  into Eqs. (12)–(15) and (31) and then write for each approximation  $\chi$  as function of  $\phi_A$ . In Fig. 7 the results for infinitely long chains in a monomeric solvent are compared for all approximations. Taking the most accurate equation [the underestimating Eq. (12)] as the reference, it is concluded that our stationary dynamics approach yields the best approximations also for  $N_A \rightarrow \infty$ .

### C. Symmetric multicomponent blends

In Fig. 8 we compare our approximation [Eq. (41)] with the exact results [Eq. (40)] for two-phase regions in symmetrical three-component blends. The smaller  $\chi N$ , the better our approximation. The product  $\chi N$  needs to be sufficiently large for the existence of a three-phase region. Figure 9 gives the result for the lowest possible  $\chi N$ , which is  $2 \ln 4 = 2.77$  [36]. In this case there is a large discrepancy between our approximation [Eq. (39)] and the exact result [Eq. (36)], in line with the conclusion above that our model becomes worse for high  $\chi N$ .

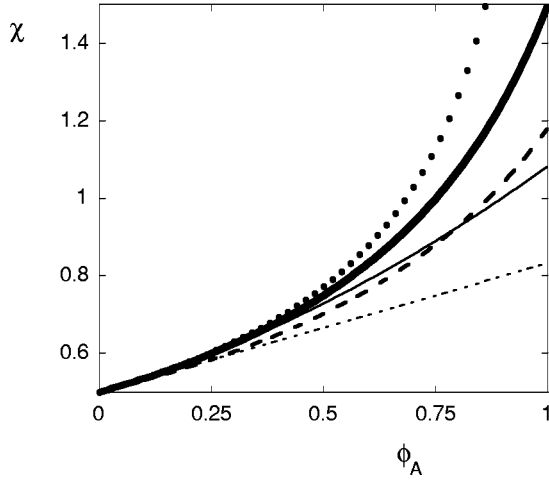


FIG. 7. Comparison of all approximations for polymer solutions:  $N_A \rightarrow \infty$ ,  $N_B = 1$ . Curves correspond to Eqs. (12)–(15) and (31) for the concentrated phase  $\beta$ , which yield  $\chi^{\text{ref}} = -(1/\phi_A^2)[\phi_A + \ln(1-\phi_A)]$  (dots),  $\chi^{\text{sol}(i)} = \frac{1}{3}\phi_A + \frac{1}{2}$  (dotted line),  $\chi^{\text{sol}(ii)} = \frac{1}{4}\phi_A^2 + \frac{1}{3}\phi_A + \frac{1}{2}$  (thin solid curve),  $\chi^{(\sqrt{3})} = \sqrt{3}/2(\sqrt{3}-\phi_A)$  (dashed curve),  $\chi^{\text{SDA}} = 3/6 - 4\phi_A$  (thick solid curve).

### V. SPINODAL COMPOSITIONS DERIVED FROM FLUX EXPRESSIONS

Spinodal compositions are strongly related to the binodal compositions. In phase diagrams, the stable and metastable mixtures are separated by the binodal line, while the metastable and unstable mixtures are separated by the spinodal line. Spinodal compositions are sometimes calculated numerically [36], although they may be calculated analytically (also for multicomponent systems) by Gibbs' determinant approach [37]. We show that exactly the same spinodal compositions are obtained by means of our flux expressions.

Suppose that at some value of  $z$  the volume fractions and their gradients are such that  $J_i(z) = 0$  for all  $i$ . (Note that we now turn to  $z$ -dependent fluxes, in contrast to the stationary fluxes considered in the search for binodal compositions.) At this  $z$  a component does not “know” in which direction it should diffuse, although there may still exist gradients in the

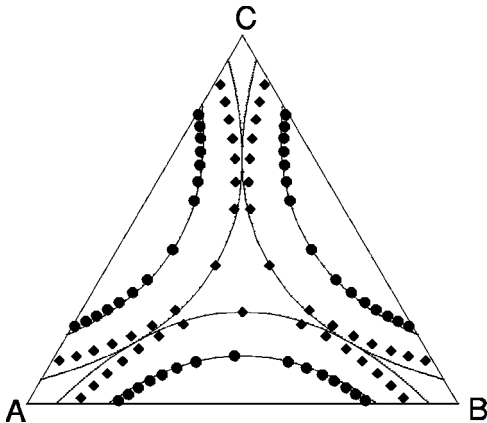


FIG. 8. Two-phase regions in symmetrical three-component blends ( $K=3$ ). Comparison of our approximation (curves) with exact results (dots:  $\chi N = 2.3$  and squares:  $\chi N = \frac{8}{3}$ ).

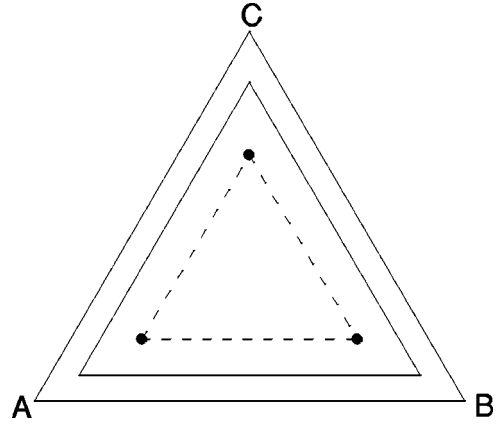


FIG. 9. Three-phase region in a symmetrical three-component blend for lowest value of  $\chi N$  leading to phase separation, i.e.,  $\chi N = 2\ln 4$  [36]. Comparison of our approximation (line) with exact results (dots).

segment chemical potentials. This indicates that the composition of the blend at  $z$  may obey the spinodal conditions. Here we show that indeed the spinodal is found by requiring that all fluxes are zero at the same position  $z$ .

We first consider binary blends. The slow- and fast-mode fluxes [Eqs. (21) and (22)] may be written in terms of only one segment chemical potential by applying the Gibbs-Duhem equation

$$J_A^s(z) = -\tilde{D}_{AA}^{s(B)}(z)\nabla\phi_A(z) = -\frac{\tilde{B}_B}{\Lambda_A(z) + \Lambda_B(z)}\Lambda_A(z)\nabla\mu_A^*(z), \quad (42)$$

$$J_A^f(z) = -\tilde{D}_{AA}^{f(B)}(z)\nabla\phi_A(z) = -\tilde{B}_B\left(\frac{\phi_A(z)}{\tilde{B}_A} + \frac{\phi_B(z)}{\tilde{B}_B}\right)\Lambda_A(z)\nabla\mu_A^*(z). \quad (43)$$

Due to the condition in Eq. (20), both components have zero flux at  $z=z'$  if

$$\tilde{D}_{AA}^{(B)}(z') = f(z')\frac{\partial\mu_A^*(z')}{\partial\phi_A} = 0. \quad (44)$$

The function  $f(z)$  is different for the slow- and fast-mode models. It is determined by the factors in front of  $\nabla\mu_A^*$  in Eqs. (42) and (43), respectively. We conclude from Eq. (44) that the fluxes are zero only for the trivial solution [ $\phi_A(z') = 0 \Rightarrow f(z') = 0$ ] or for the spinodal condition ( $\partial^2 F / \partial\phi_A^2 = 0 \Leftrightarrow \partial\mu_A / \partial\phi_A = 0$ ).

Multicomponent blends containing  $n+1$  components have  $J_i(z') = 0$  for all  $i$  if

$$|\tilde{D}| = 0. \quad (45)$$

$\tilde{D}$  is a matrix with dimensions  $n \times n$ . Its elements are the mutual diffusion coefficients  $\tilde{D}_{ij}^{(n+1)}$  for either the slow-

mode or the fast-mode model. Following the procedure for binary blends, these diffusion coefficients are written as

$$\tilde{D}_{ij}^{s(n+1)} = \Lambda_i \left( x_{ij} + \sum_{k=1}^{k=n+1} \frac{1}{\Lambda_k} \sum_{l=1}^n (\tilde{B}_{n+1} - \tilde{B}_l) \phi_l x_{lj} \right), \quad (46)$$

$$\tilde{D}_{ij}^{f(n+1)} = \Lambda_i \left( x_{ij} + \frac{1}{\tilde{B}_i} \sum_{l=1}^n (\tilde{B}_{n+1} - \tilde{B}_l) \phi_l x_{lj} \right). \quad (47)$$

These expressions are found by substituting the Gibbs-Duhem equation and the total differential of  $\mu_i^*$  into the flux equations (21) and (22). Here,  $x_{ij}$  is an element of the  $(n \times n)$ -matrix  $X_n$  and it is equal to  $(\partial \mu_i^* / \partial \phi_j)_{\phi_m \neq j}$ . After some matrix manipulations (see Appendix) it is found that the fluxes are all equal to zero if

$$|\tilde{D}^s| = \tilde{B}_{n+1} \sum_{k=1}^{n+1} \frac{1}{\Lambda_k} \left( \prod_{l=1}^n \Lambda_l \right) |X_n| = 0, \quad (48)$$

$$|\tilde{D}^f| = \tilde{B}_{n+1} \sum_{k=1}^{n+1} \frac{\phi_k}{\tilde{B}_k} \left( \prod_{l=1}^n \Lambda_l \right) |X_n| = 0. \quad (49)$$

Since all terms in the summations are definite positive, the fluxes are found to be zero only if any of the components vanish or if

$$|X_n| = 0, \quad (50)$$

which is exactly the spinodal condition for homopolymer blends containing  $n+1$  components [37]. Both diffusion mechanisms result in the same spinodal. It is easily verified that Eqs. (48) and (49) are indistinguishable if all segments have the same mobilities, that they reduce to Eq. (44) for binary blends, and that their solutions are independent of the segment mobilities.

## VI. CONCLUSIONS

The stationary dynamics approach is in principle an exact approach to obtain the compositions of coexisting phases. The binodal curves result from calculating the compositions of two distinguishable mixtures such that (i) there is no diffusion between these mixtures in the stationary state and (ii) an appropriate additional criterion is satisfied. For binary blends with  $N_A = N_B$  this additional criterion is  $\phi_A^\beta = 1 - \phi_A^\alpha$ . In our approximations we took as a general additional criterion (both for symmetrical and asymmetrical binary blends) that the stationary flux also vanishes between a binodal mixture and a critical mixture, assuming that for this

situation the chemical potential differences are approximately equal for both components.

The stationary dynamics approach becomes an approximation when the fluxes, written in terms of diffusion coefficients, are calculated analytically instead of numerically. The analytically calculated function  $z(\phi_A)$  is not an injection if  $\chi > \chi_{\text{crit}}$  (i.e., one value of  $z$  may have several values for  $\phi_A$ ) so that the analytical volume fraction profile between two mixtures is necessarily unrealistic. The expressions for the diffusion coefficients require a choice for the diffusion mechanism as well as a choice for the chemical potentials as a function of the volume fractions. These choices determine whether an analytical approach is possible or not, and the diffusion mechanism determines the accuracy of the approximated binodals, although the numerical results will always remain exact. The slow- or fast-mode diffusion mechanism in combination with the Flory-Huggins chemical potential yields an analytical approximation for the binodals when all segments have the same mobilities. This approximation for symmetrical blends ( $N_A = N_B$ ) is equal to the root-three approximation, and more accurate than the van der Waals approximation. For blends with  $N_A \neq N_B$ , our approximation is more accurate than the root-three rule as to the composition of the phase that is relatively rich in the longer chains, and comparable as to the other (diluted) phase. Our stationary dynamics approximation is also more accurate than the approximations for polymer solutions obtained by assuming that the dilute phase is essentially pure solvent. The stationary dynamics approach also yields approximations for coexisting phases in symmetrical multicomponent systems, but the accuracy decreases as the number of coexisting phases increases. Our approximations may serve as good initial guesses for the search of coexisting phases by numerical calculations or simulations. Probably, the stationary dynamics approach may also yield analytical approximations if it is combined with other diffusion mechanisms than the fast- or slow-mode mechanisms or when it is applied to another chemical potential than the Flory-Huggins potential.

We also analyzed the fast- and slow-mode flux expressions for a specific nonstationary situation. If two mixtures have arbitrary compositions, it may occur that all fluxes are zero at some moment  $t^*$  at some place  $z^*$  between these mixtures. This occurs if the composition at  $t^*$  and  $z^*$  corresponds to a spinodal composition. Therefore, the spinodal compositions may be calculated for systems with  $n+1$  components from the condition  $|\tilde{D}_n| = 0$ , where the matrix  $\tilde{D}_n$  contains  $n \times n$  diffusion coefficients  $\tilde{D}$ . Both the slow-mode and the fast-mode models yield exactly the same spinodal as calculated by Gibbs' condition  $|X_n| = 0$ , with elements  $x_{ij} = \partial \mu_i^* / \partial \phi_j$ .

## ACKNOWLEDGMENT

This research was financially supported by the Council for Chemical Sciences of the Netherlands Organization for Scientific Research (CW-NWO).

APPENDIX: CALCULATION OF  $|\tilde{D}|$ 

Using Eqs. (46) and (47), we have for  $|\tilde{D}|$

$$|\tilde{D}^s| = \left( \prod_{l=1}^n \Lambda_l \right) |X_n + Y_n|, \quad (\text{A1})$$

$$|\tilde{D}^f| = \left( \prod_{l=1}^n \phi_l \right) |W_n X_n + Z_n|. \quad (\text{A2})$$

The subscript  $n$  refers to the dimension of the square matrices. The matrices  $W_n$ ,  $X_n$ ,  $Y_n$ , and  $Z_n$  have elements defined by

$$w_{ii} = \tilde{B}_i, \quad w_{ij} = 0 \forall j \neq i, \quad (\text{A3})$$

$$x_{ij} = \left( \frac{\partial \mu_i^*}{\partial \phi_j} \right)_{\phi_{m \neq j, n+1}}, \quad (\text{A4})$$

$$y_{ij} = \sum_{k=1}^{n+1} \frac{1}{\Lambda_k} \sum_{l=1}^n (\tilde{B}_{n+1} - \tilde{B}_l) \phi_l x_{lj}, \quad (\text{A5})$$

$$z_{ij} = \sum_{l=1}^n (\tilde{B}_{n+1} - \tilde{B}_l) \phi_l x_{lj}. \quad (\text{A6})$$

Note that all rows of  $Y_n$  are identical, which is also the case for  $Z_n$ .

We define the matrix  $A_n(k, l)$  as the one that is obtained by replacing rows  $k$  and  $l$  in  $A_n$  with the corresponding rows of matrix  $B_n$ . For example, matrix  $A_4(1, 2)$  is identical to matrix  $B_4(3, 4)$ . From  $|A_n + B_n| = \sum_{k=1}^n (a_{1k} + b_{1k}) |(A_{1k})_{n-1} + (B_{1k})_{n-1}|$  it can be shown by induction that  $|A_n + B_n|$  may be calculated as

$$|A_n + B_n| = |A_n| + |B_n| \quad \text{for } n=1 \quad (\text{A7})$$

$$|A_n + B_n| = |A_n| + |B_n| + |A_n(1)| + |B_n(1)| \quad \text{for } n=2 \quad (\text{A8})$$

$$\begin{aligned} |A_n + B_n| &= |A_n| + \sum_{i_1=1}^n |A_n(i_1)| + \sum_{i_2=1}^{n-3} \sum_{i_1=i_2+1}^n |A_n(i_2, i_1)| \\ &+ \sum_{i_3=1}^{n-4} \sum_{i_2=i_3+1}^{n-3} \sum_{i_1=i_2+1}^n |A_n(i_3, i_2, i_1)| + \dots \\ &+ \sum_{i_1=n-2}^n |A_n(1, 2, 3, \dots, n-3, i_1)| + |B_n| \\ &+ \sum_{i_1=1}^n |B_n(i_1)| + \dots \\ &+ \sum_{i_1=n-2}^n |B_n(1, 2, 3, \dots, n-3, i_1)| \quad \text{for } n \geq 3. \end{aligned} \quad (\text{A9})$$

We will focus on the most complex systems with  $n \geq 3$ . Fortunately, most terms in Eq. (A9) vanish if this equation is applied to  $|X_n + Y_n|$  or to  $|W_n X_n + Z_n|$  [the determinants in Eqs. (A1) and (A2)]. This is due to the fact that  $|A_n| = 0$  if  $A_n$  has at least two identical rows. Applying Eq. (A9) we obtain for  $|\tilde{D}|$

$$|\tilde{D}^s| = \left( \prod_{l=1}^n \Lambda_l \right) \left( |X_n| + \sum_{i_1=1}^n |X_n(i_1)| \right) \quad (\text{A10})$$

$$|\tilde{D}^f| = \left( \prod_{l=1}^n \phi_l \right) \left( |W_n X_n| + \sum_{i_1=1}^n |(WX)_n(i_1)| \right). \quad (\text{A11})$$

Eqs. (48) and (49) are now readily computed by substituting

$$|X_n(i_1)| = \left( \sum_{k=1}^{n+1} \frac{1}{\Lambda_k} \right) (\tilde{B}_{n+1} - \tilde{B}_{i_1}) \phi_{i_1}, \quad (\text{A12})$$

$$|(WX)_n(i_1)| = \left( \prod_{l=1}^n \tilde{B}_l \right) \frac{1}{\tilde{B}_{i_1}} (\tilde{B}_{n+1} - \tilde{B}_{i_1}) \phi_{i_1}, \quad (\text{A13})$$

into Eqs. (A10) and (A11).

- [1] J.J. De Pablo, Q. Yan, and F.A. Escobedo, *Annu. Rev. Phys. Chem.* **50**, 377 (1999).  
 [2] A.Z. Panagiotopoulos, *Mol. Phys.* **61**, 813 (1987).  
 [3] A.Z. Panagiotopoulos, N. Quirke, M. Stapleton, and D.J. Tildesley, *Mol. Phys.* **63**, 527 (1988).  
 [4] A.D. Mackie, A.Z. Panagiotopoulos, and S.K. Kumar, *J. Chem. Phys.* **102**, 1014 (1995).  
 [5] A. Poncela, A.M. Rubio, and J.J. Freire, *J. Chem. Phys.* **114**, 8174 (2001).  
 [6] M. Laso, J.J. De Pablo, and U.W. Suter, *J. Chem. Phys.* **97**, 2817 (1992).  
 [7] J.I. Siepmann, S. Karaborni, and B. Smit, *Nature (London)* **365**, 330 (1993).  
 [8] F.A. Escobedo, *J. Chem. Phys.* **113**, 8444 (2000).

- [9] J.K. Brennan and W.G. Madden, *Macromolecules* **35**, 2827 (2002).  
 [10] D.A. Kofke, *Mol. Phys.* **78**, 1331 (1993).  
 [11] D.A. Kofke, *J. Chem. Phys.* **98**, 4149 (1993).  
 [12] M. Mehta, D.A. Kofke, *Chem. Eng. Sci.* **49**, 2633 (1994).  
 [13] Q. Yan, H. Liu, Y. Hu, *Macromolecules* **29**, 4066 (1996).  
 [14] T. Chen, H. Liu, and Y. Hu, *Macromolecules* **33**, 1904 (2000).  
 [15] W.G. Madden, A.I. Pesci, and K.F. Freed, *Macromolecules* **23**, 1181 (1990).  
 [16] A.Z. Panagiotopoulos, V. Wong, and M.A. Floriano, *Macromolecules* **31**, 912 (1998).  
 [17] A. Indrakanti, J. Maranas, A.Z. Panagiotopoulos, and S.K. Kumar, *Macromolecules* **34**, 8596 (2001).  
 [18] R. Shetty and F.A. Escobedo, *J. Chem. Phys.* **116**, 7957 (2002).

- [19] J.W. Kennedy, M. Gordon, and R. Koningsveld, *J. Polym. Sci., Part C: Polym. Symp.* **39**, 43 (1972).
- [20] W.W. Maurer, F.S. Bates, T.P. Lodge, K. Almdal, K. Mortensen, and G.H. Fredrickson, *J. Chem. Phys.* **108**, 2989 (1998).
- [21] S.L. Shmakov, *Polymer* **43**, 1491 (2002).
- [22] J. Dudowicz and K.F. Freed, *Macromolecules* **24**, 5076 (1991).
- [23] P.D. Gujrati and M. Chhajer, *J. Chem. Phys.* **106**, 5599 (1997).
- [24] L.A. Rodriguez-Guadarrama and V.R. Vasquez, *Fluid Phase Equilib.* **179**, 193 (2001).
- [25] S.A. Safran, *Statistical Thermodynamics of Surfaces, Interfaces, and Membranes* (Addison-Wesley, Reading, MA, 1994).
- [26] I.C. Sanchez, *Macromolecules* **17**, 967 (1984).
- [27] D. Qiwei He, S. Kwak, and E.B. Nauman, *Macromol. Theory Simul.* **5**, 801 (1996).
- [28] S.M. Scheinhardt-Engels, F.A.M. Leermakers, and G.J. Fleer, *Phys. Rev. E* **68**, 011802 (2003).
- [29] E.J. Kramer, P. Green, and C.J. Palmström, *Polymer* **25**, 473 (1984).
- [30] H. Sillescu, *Makromol. Chem., Rapid Commun.* **5**, 519 (1984).
- [31] F. Brochard, J. Jouffroy, and P. Levinson, *Macromolecules* **16**, 1638 (1983).
- [32] M.G. Brereton, E.W. Fischer, G. Fytas, and U. Murschall, *J. Chem. Phys.* **86**, 5174 (1987).
- [33] M.G. Brereton, *Prog. Colloid Polym. Sci.* **91**, 8 (1993).
- [34] T.E. Shearmur, A.S. Clough, D.W. Drew, M.G.D. Van der Grinten, and R.A.L. Jones, *Polymer* **39**, 2155 (1998).
- [35] M. Geoghegan, R.A.L. Jones, M.G.D. Van der Grinten, and A.S. Clough, *Polymer* **40**, 2323 (1999).
- [36] R. Horst and B.A. Wolf, *J. Chem. Phys.* **103**, 3782 (1995).
- [37] J. W. Gibbs, *The Scientific Papers of J. Willard Gibbs* (Ox Bow Press, Woodbridge, CT, 1993), Vol. I.